

Technetium-94m-Teboroxime: Synthesis, Dosimetry and Initial PET Imaging Studies

R. Jerome Nickles, Adrian D. Nunn, Charles K. Stone and Bradley T. Christian

Departments of Medical Physics, Medicine (Cardiology) and Radiology (Nuclear Medicine), University of Wisconsin, Madison, Wisconsin and Bristol-Myers Squibb, New Brunswick, New Jersey

Technetium-94m ($T_{1/2} = 53$ min) allows the *in vivo* study of technetium radiopharmaceuticals with positron emission tomography (PET). PET provides a quantitative assay of radioactivity with excellent temporal and spatial resolution, revealing biodistributions that were previously available only through *in vitro* assay methods. Technetium-94m, produced by the proton irradiation of natural molybdenum on an 11 MeV cyclotron, was extracted with an electrochemical etching technique. Technetium-94m-pertechnetate was prepared to make the myocardial perfusion agent teboroxime in an identical manner as $^{99m}\text{TcO}_4^-$. The increased absorbed radiation dose requires a sevenfold reduction in administered activity compared to ^{99m}Tc -teboroxime. Eleven clinical PET studies were performed and visually compared to ^{13}N -ammonia. The clearance half-time for ^{94m}Tc -teboroxime was ≈ 8 min, with a peak myocardial extraction of $\approx 3\%$ of the injected dose into a 400-g heart. These results confirm the potential of ^{94m}Tc PET for quantitatively studying the pharmacokinetics of new, and old, technetium agents in man.

J Nucl Med 1993; 34:1058–1066

For decades, ^{99m}Tc has completely dominated the practice of radionuclide imaging. The development of new technetium compounds must make an enormous leap, from the quantitative measurement of the biodistribution in laboratory animals to the qualitative images in man. To achieve quantitative images from either dedicated single-photon emission computed tomography (SPECT) or positron emission tomography (PET), a credible attenuation correction must be incorporated. This is particularly troublesome for SPECT in the thoracic field, with irregular volumes of lung, soft tissue and bone spanning nearly a decade in density, modulating a hundredfold attenuation correction prior to backprojection. On the other hand, PET can, and indeed must, measure the true attenuation correction from a coincidence transmission image. Even at 511 keV, this correction is of the order of ten in the chest, but its rigorous measurement allows the transverse section images to be directly expressible as μCi of activity per cm^3 of tissue.

Received Oct. 2, 1992; revision accepted Mar. 18, 1993.

For correspondence or reprints contact: Prof. R.J. Nickles, Department of Medical Physics, 1530 Medical Science Center, University of Wisconsin Medical School, 1300 University Ave., Madison, WI 53706.

This is essential for dosimetry estimates, for modeling and for understanding structure/function relationships of the radiopharmaceutical. This work would extend the same opportunity to the technetium chemist. PET will allow the basic quantitative pharmacokinetic studies of the new technetium-labeled compounds to be performed in man, allowing these agents to be understood in the same sense as the accepted flow agents, radiolabeled microspheres or H_2^{15}O . Positron tomography, by approaching the goal of quantitative *in vivo* autoradiography, eases the transition from laboratory animals to man in the developmental phase of a radiopharmaceutical.

Recently, a new class of lipophilic technetium agents (teboroxime and sestamibi) has been developed to assess perfusion of the heart. These agents derive their initial uptake kinetics from their high lipid partition characterized by octanol/saline log K values ≈ 4 . However, despite their similar lipophilicity, teboroxime is neutral while sestamibi is cationic. The two compounds differ in myocardial extraction and retention in isolated and intact cardiac preparations. In this paper, we describe the production of the positron emitter ^{94m}Tc as $^{94m}\text{TcO}_4^-$, the coordination into teboroxime, dosimetry calculations and the examination of the ^{94m}Tc -teboroxime in a limited number of subjects.

MATERIALS AND METHODS

Production

Technetium-94m is a 53-min positron emitter (2) which decays to several gamma-emitting, excited states in ^{94}Mo . It is produced, along with other technetium isotopes listed in Table 1, by the irradiation of natural molybdenum by 11 MeV protons on the UW Medical Physics CTI cyclotron. Table 1 lists the reaction, half-life, natural abundance of the pertinent molybdenum isotope, Q -value, "signature gamma" energy and representative yields, A_{EOSB} and $A_{\text{practical}}$. The first of these, A_{EOSB} , is the activity at end of saturated bombardment of a 0.1-mm (2.8 MeV) thick, natural molybdenum target with $1 \mu\text{A}$ of 11 MeV protons. The energy averaged (p,n) reaction cross section in passing through this 2.8-MeV thick target can be calculated by dividing the particular A_{EOSB} ($\text{mCi}/\mu\text{A}$) by the natural abundance of the appropriate molybdenum target isotope and multiplying by 9.5 mbarn/ $\text{mCi}/\mu\text{A}$.

The activity assay of the various technetium activities following an irradiation of known charge ($Q = f \text{ idt}$) makes use of a high-resolution, germanium gamma spectrometer ($\approx 40 \text{ cm}^3$; $\Delta E \approx 2 \text{ keV}$ at 1333 keV) efficiency-calibrated against known standards.

TABLE 1
Technetium Activation Products Resulting from Irradiation of Natural Molybdenum with 11-MeV Protons

Reaction	T _{1/2}	Abund	β ⁺ (%)	O	E _γ	A [†] _{EOSB}	A _{practical}
⁹² Mo(p,n) ⁹² Tc	4 mo	14.8%	92%	-8.8	1510 keV	1.0 mCi/μA	0.003 mCi
⁹⁴ Mo(p,n) ^{94m} Tc	53 mo	9.2%	72%	-5.1	1522 [*]	3.4	31
⁹⁴ Mo(p,n) ⁹⁴ Tc	4 hr	9.2%	11%	-5.0	702	0.76	3.1
⁹⁵ Mo(p,n) ⁹⁵ Tc	20 hr	15.9%	0%	-2.4	766	4.3	5.0
⁹⁵ Mo(p,n) ^{95m} Tc	61 d	15.9%	0.3%	-2.5	204	1.5	0.025
⁹⁶ Mo(p,n) ⁹⁶ Tc	4 d	16.7%	0%	-3.7	778	10.0	2.4

^{*}Both ^{94m}Tc and ⁹⁴Tc decay with the emission of an 871-keV gamma, requiring the use of a unique gamma ray listed here for identification and activity assay.

[†]The reaction cross section (in mb), averaged across this 2.8-MeV thick target, is the saturated activity A_{EOSB} divided by the isotopic abundance and multiplied by 9.5 mb/mCi/μA.

Since both isomeric levels and their respective ground states (e.g., ^{94m}Tc/⁹⁴Tc) are directly produced in proton irradiation and can pass through common gamma de-excitation pathways (e.g., the 871-keV level in ⁹⁴Mo), the assay of activities hinges on the spectroscopy of unshared "signature gammas" that are unique to a particular decay. Typical spectra are shown at various times from minutes to several months postirradiation (Fig. 1).

The energy dependence of the various (p,n) reaction cross sections was studied in a stacked-foil experiment. A sandwich of twenty 25-μm molybdenum foils was irradiated, and the production of six technetium radioisotopes measured with the germanium detector described above, as the beam energy is degraded from 11 MeV to zero. From these thin target data, it is apparent that a 53-min irradiation from 11 MeV > E_p > 8 MeV will favor the radionuclidic purity of ^{94m}Tc, anticipating a similar 1-hr workup time for labeling. This is listed as A_{practical} in the last column of Table 1, as the activities of the various technetium isotopes that can be expected 1 hr after a 53-min irradiation of a 102-mg/cm² natural molybdenum foil with 40 μA of 11 MeV protons. The total mass of technetium isotopes produced in the practical irradiation of Table 1 amounts to roughly 100 pmole, resulting in a specific activity of ≈200 Ci/μmole (7.4 TBq/μmole), comparable to the specific activity from a ^{99m}Tc generator, eluted daily.

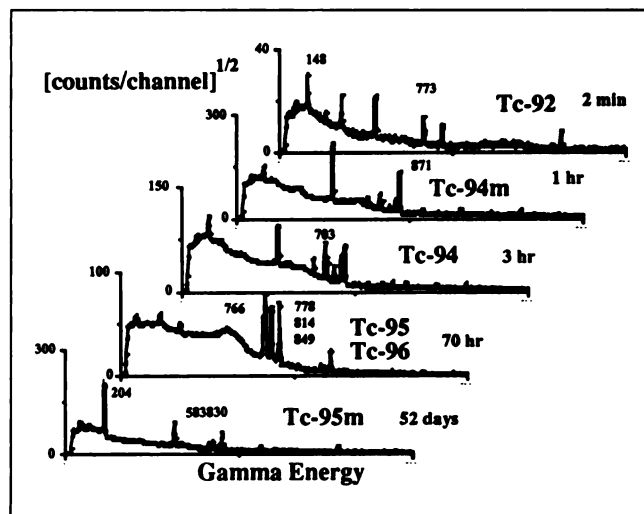


FIGURE 1. A succession of high-resolution gamma ray spectra from a natural molybdenum target taken at the stated times postirradiation.

Extraction of TcO₄⁻

The rapid dissolution of the molybdenum target foil (≈100 mg, 0.1-mm thick, Aldrich Chemical Corp) is performed electrochemically (3). The glassy carbon cell (Fig. 2) acts as the cathode which contains the electrolyte (3:1 1N HCl/30% H₂O₂). It is vibrated in an ultrasonic ice bath during the electrolysis (3 min, 3 volts, ≈5 A/cm²) to free surfaces of gas bubbles. Following dissolution, the electrolyte is made basic with NaOH and the radioactive TcO₄⁻ is extracted into an equivolume of methyl ethyl ketone (MEK) (4). Successive washings with fresh 1 N NaOH reduce molybdenum and H₂O₂ levels by 1–2 decades per wash, as evidenced by colorimetric assays of acidic potassium ethyl xanthate (5) and peroxide test strips, respectively.

A separate study of the MoO₄⁻ partition between base and MEK was performed using the 7-hr isomer ^{93m}Mo, which was produced by proton irradiation of a niobium foil. Here, the electrochemistry results in ^{93m}Mo-molybdate, which favors the aqueous fraction in a 30:1 ratio over MEK. Four solvent extractions suffice to reduce Mo by >10⁵ (100 mg ≥ 1 μg) to the ppm level, while leaving (0.9)⁴ ≈65% of the technetium activity remaining at 30–40 min post-EOB. The technetium bearing MEK fraction is then blown dry in a helium stream at 100°C and taken up in 1 ml of 0.9% physiological saline. This activity (pH ≈7) proves to be >99% TcO₄⁻ as shown by thin-layer chromatography (TLC) (silica gel, MEK/MeOH 1:1, R_f = 0.9) and high-performance liquid chromatography (HPLC). Although careful attention to good laboratory technique has been practiced up to this point, the TcO₄⁻ solution is next passed through a sterile, 0.22-μm filter (Millipore, Millex GV) prior to introduction into any commercial kit preparation. Sterility and pyrogenicity tests of the ^{94m}TcO₄⁻ at this stage assures us that we are in the same pharmaceutical position as one would be prior to introducing generator-derived ^{99m}TcO₄⁻ into the same kit.

Synthesis of ^{94m}Tc-Teboroxime

Commercial CardioTec kits were obtained from Squibb and authorized with full approval of the University of Wisconsin/Wm S. Middleton Veteran's Administration Hospital Radioactive Drug Research Committee for ^{94m}Tc labeling for human use. Typically, 20–30 mCi (≈1 GBq) of ^{94m}TcO₄⁻ in 1 ml of 0.9% physiologic saline was introduced into the CardioTec kit, shaken and heated to 100°C in a dry heating block for 15 min, in the manner described in the package insert. At the end of synthesis, radiochemical purity in excess of 96% was shown by both standard TLC (Whatman 31 ET Chrom, mobile phases of saline and

saline/acetone) as well as HPLC on a C-8 Econosil 10- μ m column (65% MeCN/35% 0.1 M sodium citrate buffer, pH = 5, 1.5 ml/min, retention time = 12 min) (Fig. 3). Sterility and apyrogenicity of the final preparation was tested on each batch.

Dosimetry

The absorbed radiation dose to the patient from technetium labeled with the five technetium isotopes remaining at the time of injection (\approx 53 min post-EOB) was estimated. This was first done by building on the extensive (6) biodistribution literature acquired with ^{99m}Tc -teboroxime and then refined by incorporating the PET-based experimental findings of this study. Following the MIRD approach, these estimates break down into the computation of two factors: the cumulative activity, A , and the absorbed dose S-factor, which enters into the product $D = A \times S$.

First, the cumulative activity $A = \int a(t) dt$ is calculated by running the ICRP model (7) of the gastrointestinal (GI) tract as a STELLATM (Lyme, NH) program to predict the time course, $a(t)$, of each technetium radioisotope in its passage through each target organ along the excretory route. The initial conditions of this model incorporate the experimental finding ($n = 6$) that the blood pool is rapidly cleared, with $14.6\% \pm 3.1\%$ of the injected dose appearing as the peak activity in the patients' liver at 5 min postinjection. The ICRP model links the liver (gallbladder), small intestine (SI), upper large intestine (ULI) and lower large intestine (LLI) in a catenary pathway with realistic masses, contents, wall thickness and transit times. The remaining 85% of the injected activity is assumed to be uniformly distributed about the whole body and fixed, a patently pessimistic assumption. This results in a 5 (technetium isotopes) \times 4 (source organs) matrix of functions, $a(t)$, whose time integrals $A = \int a(t) dt$ ($\mu\text{Ci-hr}$ or Bq-hr) are the cumulative activities needed for MIRD computation. These cumulative activities, A (Table 2), are normalized to the actual activity that would accompany a 1-mCi (37 MBq) injection of ^{94m}Tc made from natural molybdenum at injection 1 hr post-EOB. Technetium-92 can be neglected since it will have decayed away by 53 min post-EOB.

Second, since the S-factors of these technetium isotopes have not been calculated from the photon transport through standard man, they must be estimated by interpolation between S-factors of radioisotopes of similar radiation properties that have been tabulated (8). The smooth energy dependence of the mass attenuation coefficient $\mu(E)$ modulates the absorbed dose fraction Φ , which is a double integral over the source and target volumes

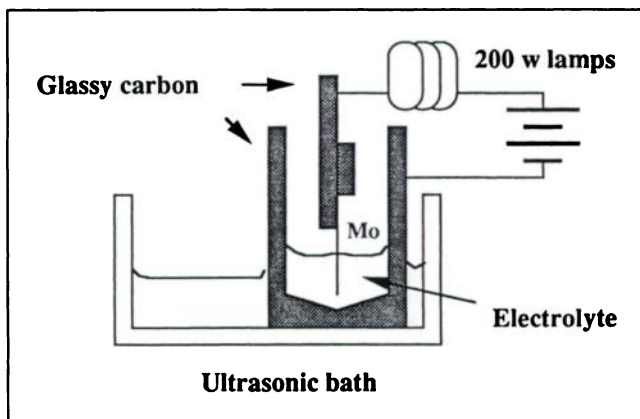


FIGURE 2. Schematic diagram of the electrochemical cell used to rapidly dissolve the irradiated molybdenum foil target.

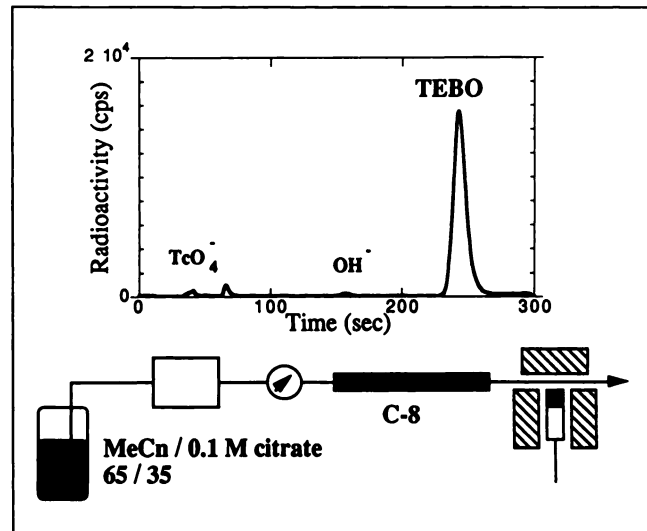


FIGURE 3. Typical radiochromatogram of ^{94m}Tc -teboroxime under conditions stated in the text.

$$\Phi = \iint B(\mu(E)) \exp(-\mu(E)\Delta r) / (\Delta r)^2 dV_i dV_j$$

that encompasses the build-up factor, B , the exponential attenuation, $\exp(-\mu\Delta r)$ and $1/\Delta r^2$ ($\Delta r = r_i - r_j$), interorgan separation. This allows an ordered expansion to describe the absorbed gamma dose S-factor to target organ j from the cumulative activity of each technetium isotope, k , in source organ, i . To the first order, S-factors can be estimated from the MIRD tables (8) by constructing "mock technetium" equivalents listed in the last column of Table 2. The conversion factors (e.g., $^{94m}\text{Tc} = 0.64 \times ^{82}\text{Rb}$) are simply based on $\sum E_k n_k \Phi_k$ weighting by the product of the energy, E_k , branching ratio, n_k , and absorbed dose fraction, Φ_k . The GI tract components are taken here to be 2-kg flat ellipsoids for this calculation. This approach is readily verified by checking, for example, the tabulated S-factors for the liver-to-small intestine:

$$S(^{11}\text{C}) = 1.2 \times 10^{-5} \approx 2 \times S(^{85}\text{Sr}) \\ \approx \{ \sum E_k n_k \Phi_k(^{11}\text{C}) / \sum E_k n_k \Phi_k(^{43}\text{K}) \} \times S(^{43}\text{K}).$$

The dosimetry calculations, $D = A \times S$, must link not only the key organs along the GI tract but also their radiation effect on such targets as blood-forming organs, testes or uterus, lens of the eye and whole body. This requires computation of the 4 (source organs) \times 8 (target organs) = 32 S-matrix elements for each of the five technetium isotopes present at injection which form a $4 \times 8 \times 5$ tensor array.

By factoring the dosimetry problem into:

- the cumulative activity calculation deriving $A = \int a(t) dt$ from a credible GI model anchored to measured human biodistributions,
- the straightforward interpolation of the relevant S-factors accurate to within 10%,

the product of the (5×4) A-matrix with the $(4 \times 8 \times 5)$ S-tensor array yields the predicted dose D . This dose tensor is collapsed by summing over the four source organs to yield Table 3, which explicitly breaks out the dose to eight organs from the five technetium isotopes accompanying a 1-mCi (37 MBq) injection of ^{94m}Tc . This matrix is further collapsed by summing over technetium

TABLE 2
Cumulative Activity ($\mu\text{Ci-hr}$)

Isotope	Activity*	Liver	SI	ULI	LLI	Mock Tc†
^{94m}Tc	1000 μCi	174	84	24	2	$0.64 \times ^{82}\text{Rb}$
^{94}Tc	100	18	18	21	15	$0.78 \times ^{52}\text{Mn}$
^{95}Tc	170	31	85	199	200	$1.35 \times ^{86}\text{Sr}$
^{95m}Tc	0.8	0.1	.05	2	4	$^{99m}\text{Tc} + ^{86}\text{Sr}$
^{98}Tc	77	14	42	137	212	$5 \times ^{86}\text{Sr}$
$^{99m}\text{Tc}^\ddagger$	1000 μCi	396	826	1206	592	^{99m}Tc

*Activity in $\mu\text{Ci/mCi}$ of ^{94m}Tc at injection.

†Simulates the dose effects of the particular technetium isotope, as $S(^{94m}\text{Tc}) \approx 0.64 \times S(^{82}\text{Rb})$ for liver \geq SI. See text.

‡Technetium-99m is not present in a ^{94m}Tc injection, but is included for comparison.

tium isotopes to yield the total absorbed dose by organ. This column is listed as ALL Tc and compared to the corresponding dose values expected for 1 mCi (37 MBq) of ^{99m}Tc -teboroxime using the same GI model. The close agreement between the ^{99m}Tc -teboroxime dose estimates based on this ICRP model-based approach and the results (9) of measured kinetics in man is reassuring and shows that the critical organs are the intestinal walls which were irradiated by their own contents.

Two immediate conclusions can be drawn concerning the absorbed dose to the large intestine, the critical organ for both teboroxime labeled with ^{99m}Tc and our ^{94m}Tc mixture. First, the eightfold greater radiation dose from ^{94m}Tc will require an eightfold reduction in administered activity. For this reason, with natural molybdenum as the target material and a 5-rem critical organ limit, our figures show that 4 mCi (148 MBq) of ^{94m}Tc or 30 mCi (1.1 GBq) of ^{99m}Tc -teboroxime are allowable for single-dose, cardiac perfusion studies. Second, the irradiation of isotopically-enriched ^{94}Mo would eliminate some of the long-lived radionuclidic impurities (^{95}Tc , ^{95m}Tc and ^{96}Tc), although the ground state ^{94}Tc is unavoidable. Summing over the first two columns of Table 3 shows that the critical organ now becomes the liver and that the reduction in absorbed radiation dose would permit a fourfold scale up in administered activity. Work is underway at this laboratory (10) to develop targetry and recycling procedures to conserve this precious (\sim \\$6/mg) enriched material.

Instrument Calibration

The emergence of ^{94m}Tc into the field of quantitative in vivo measurement demands the development of calibration procedures, both for its assay in "dose calibrators" as well as the

positron scanner. This exercise must be logically self-consistent, but not circular. This is made more difficult in our case since:

1. There is always a changing mixture of technetium isotopes, $A(t) = \sum A_i(0) \exp(-\lambda_i t)$, with well-known half-lives ($\ln 2/\lambda_i$), but initial activities, $A_i(0)$, that depend on irradiation details (target thickness, beam current history, etc.).
2. An ionization chamber dose calibrator anticipates a pure radionuclide, which is not possible even with enriched ^{94}Mo targets. As a result, the only utility of a dose calibrator is to perform *relative* assays of the splitting of a sample ($\text{Total} = A + B + C + \dots$) into separate known fractional aliquots. Thus, a calibration constant or decay correction is not needed.
3. The high-resolution gamma spectra from an efficiency calibrated germanium detector *can* assay ^{94m}Tc activity, although even this is not a trivial measurement. The major gamma line (871 keV) is common to both ^{94m}Tc and the ^{94}Tc ground state formed directly during irradiation of natural or enriched molybdenum. Nonetheless, these gamma spectra, unraveled by the unshared gamma lines at 1,522 keV (4.8%) and 1,868 keV (6.1%) for ^{94m}Tc and 702 keV (100%) for ^{94}Tc , are the linch-pin in a quantitative assay. The time-resolved spectra (Fig. 1) lead to an absolute assay of each radionuclide in μCi (Bq) based on the literature branching ratios (2).
4. The PET scanner, on the other hand, responds to positrons from any source. The calibration constant relating absolute μCi (Bq) to ECAT cps/pixel (a standard, but unfortunately misleading notation) is dependent on the isotope (β^+

TABLE 3
Absorbed Dose Estimates (mrad) from Various Technetium Isotopes Accompanying 1 mCi of ^{94m}Tc at Injection

Target organ	^{94m}Tc (1000 μCi)	^{94}Tc (100 μCi)	^{95}Tc (170 μCi)	^{95m}Tc (0.8 μCi)	^{98}Tc (77 μCi) [*]	All	^{99m}Tc	Ref. 9
Liver	236	35	55	15	409	750	30	62
SI	212	49	94	17	552	924	106	108
ULI	157	57	125	17	630	986	196	123
LLI	64	51	133	17	752	1017	137	87
WB	50	23	43	14	330	460	20	17
Gonads	52	44	45	17	425	583	12	10
Lens	52	18	38	17	425	550	12	—
Marrow	52	17	50	17	343	479	29	17

*Injected activity.

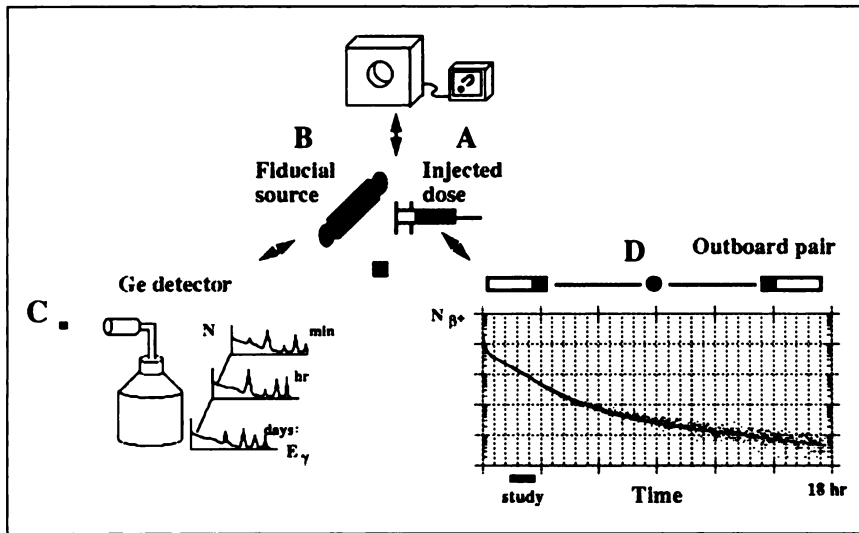


FIGURE 4. Schematic flow chart of the ^{94m}Tc calibration strategy, where the whole batch is partitioned into four samples of known relative activities. Sample A is the injected fraction; B is a fiducial marker source included in the PET scanner field of view; C is assayed by the intrinsic germanium spectrometer for absolute activity calibration and D is data-logged in an outboard NaI(Tl) coincidence pair with β^+ sensitivity that is a constant fraction of the PET scanner, for later decay correction.

branching ratio) and energy thresholds. Although ^{94m}Tc is the dominant positron emitter, ^{94}Tc impurities could cause problems in the late phases of a scan, if they were “corrected” by erroneous calibration constants of the dose calibrator, the PET scanner and decay rate.

The selectivity of the PET scanner to positron decay buried amid a background of coincident gammas has been carefully matched in a mock PET scanner dedicated to this project. It consists of a pair of 5×5 cm NaI(Tl) detectors separated by 1 m on the bench top. This “outboard pair” detects colinear, 511 keV photoevents in a 15-nsec (FWHM) timing aperture with a constant positron sensitivity relative to the PET scanner and the same three decade rejection of noncolinear events. The coincidence counting rate of a centered test source of ^{94m}Tc is data logged at 1-min intervals, and is used for all positron-specific decay corrections. The sensitivity of this pair is extremely position-dependent for small sources, but invariant to plane sources extending beyond the 5-cm diameter field of view. This outboard pair is a fixed instrument, dedicated to these studies, with energy and timing windows carefully held constant as shown with long-lived ^{22}Na and ^{68}Ge sources.

Figure 4 shows this logical flow that propagates the absolute calibration from known sources to detectors and allows the PET scanner to assay ^{94m}Tc directly in microcuries. Briefly, upon reaching the point in the chemistry where the TcO_4^- is isolated, the total activity is separated into four (A, B, C, D) separate aliquots of carefully measured relative activity in the approximate ratio of (100:10:1:1). The largest fraction A is used to produce ^{94m}Tc -teboroxime. Later, a measured portion of this aliquot will be injected into the patient. The second aliquot B is introduced into a 1-cm diameter, 50-cm long fiducial source volume, mounted on the scanner bed beneath the cushioned back of the patient. This source is easily resolved from the patient in the thoracic field of view and has a diameter roughly twice the scanner resolution to minimize partial volume effects in the assay of its activity. The third fraction C is sequentially analyzed with the high purity germanium spectrometer for absolute assay of all technetium activities in μCi (Bq), while the fourth fraction D fills an extended source and is placed between the outboard pair for an independent assay of positron activity at high temporal frequency (1 min^{-1}) for any decay correction.

In this way, it is possible to avoid any reference to Capintec

calibration constants, ECAT scale factors, decay rates or scanner losses, all of which propagate systematic errors in the analysis of the PET images. This exercise is easy to bungle in the clinical setting, but with proper attention to transmission scanning of the cold fiducial volume, rigidly mounted to avoid registration artifacts, and judicious selection of the afterload source strength, a more serious nest of problems is averted. It is important to remember however, that by basing our measurements of observed ratios (myocardial tissue “ECAT number”-to-fiducial “ECAT number” against total injected activity-to-fiducial activity in its known volume) we are determining the *fraction of the injected dose* that is taken up in a unit volume of myocardial tissue. Organ-specific uptake requires only multiplication by organ volume, which was taken from literature values.

Validation

This quantitation procedure was validated in an exhaustive study with 20-cm (diameter) cylindrical volume phantoms generally used to standardize scanner sensitivity with conventional PET radionuclides such as ^{18}F . Volume-matched and activity-matched phantoms were sequentially scanned and positron counted in the outboard pair over six half-lives; they were first charged with aqueous $^{18}\text{F}^-$ and then with $^{94m}\text{TcO}_4^-$. From known activities assayed by the germanium detector, the ECAT calibration factors (7.0 and $6.9 \mu\text{Ci}/\text{ml}/\text{cps}/\text{pixel}$, respectively) were determined, although they will not be needed in image quantitation.

The results of these measurements are shown in Figure 5, which tracks the normalized counting rates from the PET scanner (open circles) and the outboard pair (dots) for both ^{18}F and ^{94m}Tc over almost two decades. The ^{94m}Tc patient studies are all completed by the end of the first half-life, while the decay is effectively monoexponential with a 53-min half-life for at least three to four half-lives. The most important result, however, is that the count rate ratio of the ECAT to the outboard pair is 9.9×10^{-3} for ^{18}F and 10.5×10^{-3} for ^{94m}Tc . This is not significantly different in light of the 3% interslice differences. The equality of these scale factors between ^{18}F and ^{94m}Tc means that the outboard pair, if properly maintained, can act as a true fiducial monitor.

In summary, let C refer to the PET image-based “counting rate” per pixel integrated over the myocardial (C_m) or fiducial (C_f) regions of interest (ROIs). Let A refer to the activity in any unit, with only the dimensionless fiducial-to-injected ratio (A_f/A_{inj})

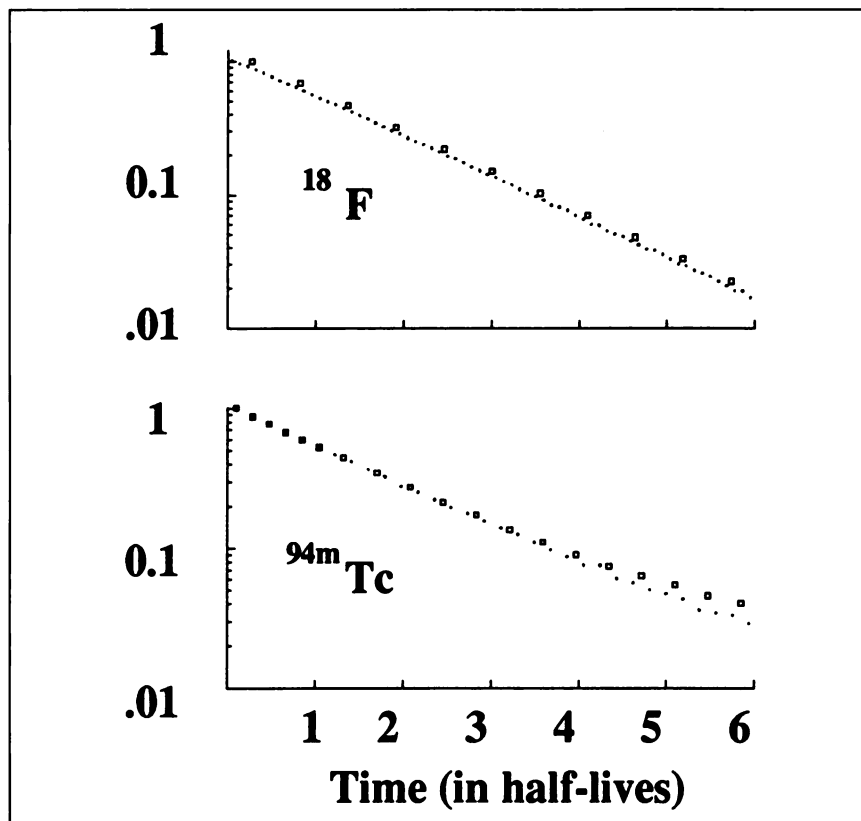


FIGURE 5. The PET scanner (open circles) and the outboard pair (dots) track the decay of both ^{18}F (upper plots) and $^{94\text{m}}\text{Tc}$ (lower plots) in a 20-cm diameter volume phantom over six half-lives. Whereas ^{18}F is rigorously monoexponential, the technetium mixture appears to be essentially pure $^{94\text{m}}\text{Tc}$ for almost four half-lives, which is long when compared to the 20-min patient study. The ratio of the PET scanner-to-outboard pair sensitivities is identical for the two radionuclides, in spite of the extensive coincident gamma traffic with $^{94\text{m}}\text{Tc}$. This establishes the calibration pathway for quantitative PET imaging with $^{94\text{m}}\text{Tc}$.

being needed. Then the fraction, f , of tracer taken up in the myocardium of volume V_m is simply:

$$f = (C_m/C_f)(A_f/A_{inj})(V_m/V_f).$$

By moving the fiducial source out of the PET scanner and into the outboard pair, only a fixed constant of proportionality is introduced. In the end, this technique does *not* involve:

1. A dose calibrator, other than to split activities into fractions.
2. A germanium detector, other than to initially identify radionuclidic impurities.
3. Any ECAT calibration factors.
4. Any published decay schemes.
5. Any irradiation or targetry details.

It *does* require a stable outboard pair, careful measurement of A_f/A_{inj} and use of $^{94\text{m}}\text{Tc}$ within the first few half-lives.

PET Imaging Characteristics of $^{94\text{m}}\text{Tc}$

The role of radiopharmaceuticals and imaging instrumentation in the diagnosis of a patient's biomedical problems has been historically arrayed as a triangular relationship to emphasize their interplay (11). This work describes $^{94\text{m}}\text{Tc}$ labeling of teboroxime in PET scanning of patients with cardiac disease. Clearly, some initial work is needed to demonstrate the PET imaging characteristics of $^{94\text{m}}\text{Tc}$ in phantoms with known radionuclide distributions. Toward this end, a Jaszczak thoracic phantom with a cardiac insert was filled with a 5:1 concentration ratio between the "myocardial tissue" doughnut and the neighboring intraventricular contents and the extracardiac "body" pool. The cardiac chamber is secured inside the chest cavity on a solid lucite support, which provides a convenient zero activity region into the image. The phantom was then sequentially filled with ^{201}Tl , $^{99\text{m}}\text{Tc}$, $^{94\text{m}}\text{Tc}$ and

^{18}F (a pure positron emitter with ideal PET imaging properties) and imaged on the appropriate scanner.

The activity and imaging time product were chosen to be ten times greater than in typical clinical studies [i.e., ^{201}Tl (3 mCi \times 30 min); $^{99\text{m}}\text{Tc}$ (30 mCi \times 30 min); $^{94\text{m}}\text{Tc}$ (4 mCi \times 30 min); ^{18}F (10 mCi \times 30 min)]. This ensured that the image sets would be realistically scaled relative to each other, but with adequate statistics to reveal the strengths of the SPECT (Trionix Triad) and PET (CTI 933/04) imaging devices viewing the respective radionuclide candidates. Figure 6 shows the result of this exercise, demonstrating that while additional coincident gamma rays in the decay of $^{94\text{m}}\text{Tc}$ add a slight mottle relative to ^{18}F , the resulting image quality is far superior to the best case with SPECT. Both SPECT and PET image sets were carefully attenuation-corrected, made possible in SPECT due to the artificial absence of low density lungs in the reconstruction field. The activity derived from the image sets in ROIs A (thoracic field = 100%), B (lucite support = 0%), C (annular myocardial tissue = 500%) and D (ventricular interior = 100%) are listed in Table 4. Spillover is evident in each case, in spite of drawing ROI borders one resolution distance inside from any edge to minimize partial volume effects.

Patient Protocol

Institutional approval* was secured for paired PET studies on normals and patients (male and female) with both $^{13}\text{NH}_3$ and $^{94\text{m}}\text{Tc}$ -teboroxime in injected activities up to 30 and 4 mCi, respectively. The synthesis of the $^{94\text{m}}\text{Tc}$ -teboroxime/ ^{13}N -ammonia

*Institutional approval from University of Wisconsin Human Subjects Committee; University of Wisconsin/Wm S. Middleton VAMC Radioactive Drug Research Committee; Wm S. Middleton VA Research and Development Committee; University of Wisconsin and Wm S. Middleton VAMC Radiation Safety Committees.

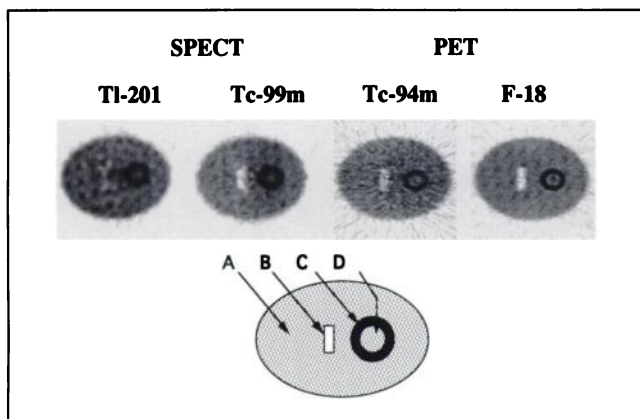


FIGURE 6. Four images of a thoracic phantom with a cardiac insert filled with ^{201}Tl , $^{99\text{m}}\text{Tc}$, $^{94\text{m}}\text{Tc}$ and ^{18}F at activities corresponding to clinically relevant doses (3, 30, 4 and 10 mCi, respectively) and tomographically imaged for statistics ten times greater than would be normally achieved in practice to better reveal the imaging characteristics of each radionuclide. The ratio of activity concentration in the myocardial wall chamber (C) to the concentration both inside (D) and outside (A) was made to be 5:1, while the dark rectangular region (B) is the lucite cardiac support representing zero activity. The measured activity concentrations, carefully derived from ROI analysis on the attenuation-corrected images, are normalized to the extracardiac region A and listed in Table 1.

pair is coordinated to minimize patient time in the scanner. The $^{13}\text{NH}_3$ "plays through." With a 20-min irradiation and 2-min synthesis, it can be made (12) and administered during $^{94\text{m}}\text{Tc}$ -teboroxime workup.

After informed consent was obtained, the scan sequence started with a brief transmission (^{68}Ge ring source) rectilinear scan, to center the seven planes of the four-ring scanner (CTI-Siemens Inc. 933/04-12) with a 52-mm total axial field of view over the desired thoracic landmarks. This is followed by a 10-min, 5-megacount transmission scan that is reconstructed immediately to reassure the clinician that patient positioning is correct. Upon completion of the transmission studies, the ammonia dose is injected in a 15-sec programmed infusion and scanned. The dynamic sequence consists of twenty-four 5-sec, four 30-sec and eight 2-min scans. On-line reconstruction confirms that the study is progressing properly. At about 40–50 min post- $^{13}\text{NH}_3$ injection, $^{94\text{m}}\text{Tc}$ -teboroxime synthesis and quality control is completed, and the dose arrives. The 15-sec infusion and 20-min scan sequence are repeated, with the subject free to leave in less than 2 hr after

TABLE 4
Spillover Results from the Thoracic Phantom

	ROI			
	A	B	C	D
Measured	(100)	(0)	(500)	(100)
^{18}F	100	11	296	146
$^{94\text{m}}\text{Tc}$	100	22	238	123
$^{99\text{m}}\text{Tc}$	100	46	306	172
^{201}Tl	100	61	221	139

Numbers in parentheses are actual concentrations.

arrival. The reconstructed image set is transmitted via EtherNet to a $\mu\text{VAX-GPX}$ workstation for ROI analysis using a flexible program (13) calling IDL (Research Systems, Denver, CO) routines. Selected images are summed and sent to a Mac IIX for 24-bit color presentation and film exposure (Still Light, American Liquid Light Inc., Torrance, CA). Finally, time-activity curves are analyzed in an effort to compare myocardial washout and blood-pool contributions of ^{13}N and $^{94\text{m}}\text{Tc}$ activities.

RESULTS

Eleven clinical studies have been completed in normals as well as patients with normal and abnormal thallium scintigrams. The results listed in Table 5 represent the last eight subjects who received the extraction quantitation described above. In this first clinical series, a broad patient population was studied. Volunteers were recruited who were normal or who were patients with coronary disease. Due to the dosimetry of $^{94\text{m}}\text{Tc}$, single studies were performed and the stress/rest selection was performed randomly. Dynamic imaging demonstrates rapid myocardial uptake and washout of $^{94\text{m}}\text{Tc}$ -teboroxime (Fig. 7).

Time-activity curves were constructed with ROIs over the septum and left ventricular blood pool. The initial portion of the myocardial time-activity curve shows a rapid decline in tissue activity with a mean half-time of 10 sec. However, much of this early clearance of teboroxime is related to spillover from rapidly declining blood-pool activity. As expected, during the initial transit of the bolus through the heart, blood-pool activity was higher than

TABLE 5
Patient Results

Study	^{201}Tl results	Washout $T_{1/2}$ (min)	Peak extraction*
P 538	Male 73; Rest, no Tl defects	11	2.5%
P 548	Male 51; Rest, small reversible inferior wall defect	7	2.9%
P 802	Male 60; Rest, no Tl defects	10	3.2%
P 832	Female 73; Rest, fixed lateral wall defect	10	4.1%
P 834	Male 55; Rest, reversible apical defect	6	4.0%
P 549	Male 42; Handgrip stress, normal	6.5	2.1%
P 780	Male 68; Adenosine stress, infero-apical defect	5	2.7%
P 812	Female 51; Adenosine stress, no Tl defect	11	3.2%

*Peak myocardial extraction averaged over the septum assuming a 400-g heart mass.

Note, the septal region was chosen for analysis to minimize motion artifacts and partial volume effects.

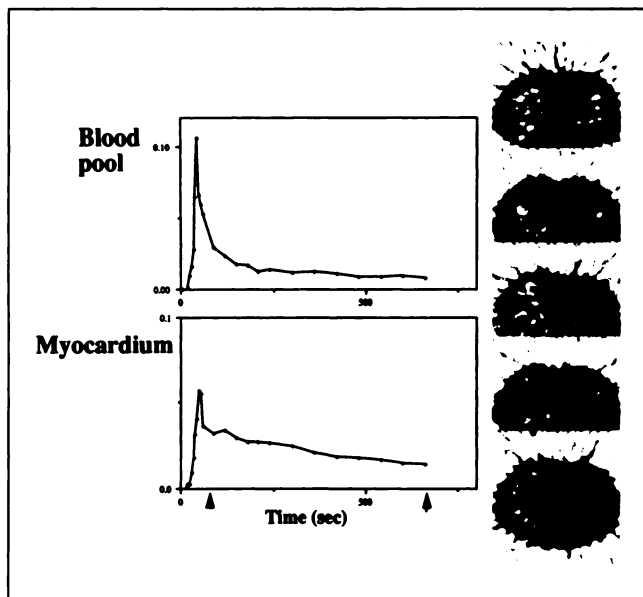


FIGURE 7. A five-slice, descending atlas of ^{94m}Tc -teboroxime myocardial images in a normal subject summed from 2 to 11 min. The accompanying time-activity curves reveal the fast blood clearance and ≈ 7 -min teboroxime washout ($T_{1/2}$) from the myocardial tissue.

myocardial activity. However, after 30 sec, this was reversed. Average half-time for myocardial washout, after clearance of the blood pool, was 8.3 min (s.d. = 2.4). At rest, the peak myocardial extraction of teboroxime was $5.2\text{--}10.2 \times 10^{-3}\%$ of the dose per gram of heart tissue, or 2.1%–4.1% ($n = 8$) of the total injected dose, assuming a heart mass of 400 g. With handgrip or adenosine stress ($n = 3$ of 8), this peak myocardial uptake was not significantly changed to within statistics.

Transaxial images summed from 2 to 12 min revealed excellent myocardial uptake of the tracer with a high target-to-background ratio as shown in Figure 8, which compares $^{13}\text{NH}_3$ and ^{94m}Tc -teboroxime images in a patient with a clear lateral wall defect. The blood-pool activity stabilized at 8 min with an activity of $0.5\text{--}0.6 \times 10^{-3}\%$ of the injected dose remaining per ml of whole blood, or 3.1–3.7% ($n = 2$) of the dose in an estimated 6-liter blood pool, as measured by germanium spectroscopy on blood samples drawn at the end of the scanning period. Since arterial samples were not drawn nor blood serum HPLC analysis performed to determine the circulating free ligand concen-

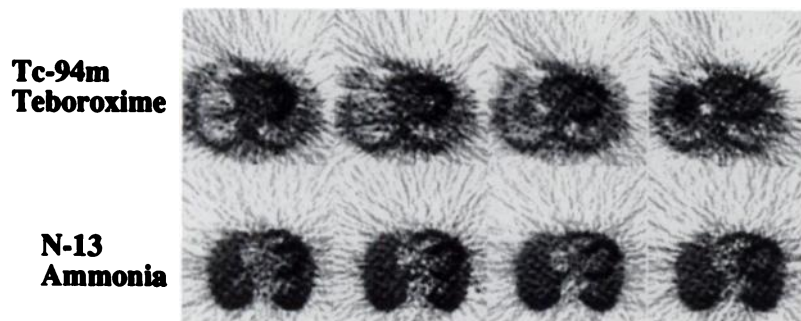


FIGURE 8. A four-image set (descending across) of $^{13}\text{NH}_3$ (lower) and ^{94m}Tc -teboroxime (upper) of a resting patient with a lateral wall defect summed from 4 to 20 min, respectively.

tration in the input function, no serious compartmental modeling of teboroxime kinetics was undertaken. However, the striking correspondence between the relative uptake between the two partially extracted agents, $^{13}\text{NH}_3$ and ^{94m}Tc -teboroxime, provides phenomenological encouragement that these agents have similar potential as regional flow tracers.

DISCUSSION

The widespread acceptance of ^{99m}Tc in clinical nuclear medicine is related to its favorable logistics and imaging characteristics. Considerable effort is being expended by numerous groups to achieve quantitative imaging of ^{99m}Tc with SPECT, even to using co-registered dual-energy CT for obligatory transmission imaging (14). Although these advances in instrumentation hold great promise for the future, the current practice of clinical ^{99m}Tc imaging is unable to assign a quantitative scale, an activity (μCi or Bq per cm^3) to the SPECT image. The positron emitter ^{94m}Tc , with its 53-min half-life and its chemical identity to ^{99m}Tc , is uniquely suited for PET studies of technetium radiopharmaceuticals. The imaging capabilities of PET, which offers quantitative in vivo assay of radioactivity at high temporal and spatial resolutions, would allow the noninvasive measurement of the biodistribution and pharmacokinetics of technetium agents in man.

In this preliminary report on the application of ^{94m}Tc to technetium radiopharmaceutical chemistry, we have described ^{94m}Tc production, extraction and coordination to teboroxime, as well as the dosimetry and the results of initial clinical studies. The perfusion agent CardioTec was chosen as the initial radiopharmaceutical to study because of its high myocardial extraction and rapid washout. In these initial studies, we were able to demonstrate a myocardial clearance half time of ≈ 8 min after an intravenous injection. This rate is similar to the clearance rate reported by Seldin et al. on anterior planar views at rest (15). The peak myocardial extraction of ^{94m}Tc -teboroxime was about 3% of the injected dose, which is consistent with the previous in vitro value of $2.3\% \pm 0.8\%$ determined in Phase I biodistribution studies of ^{99m}Tc -teboroxime (16, 17). This is lower than expected from single-pass extraction experiments in isolated hearts in which extraction rates of 96% have been found, probably due to the intravascular binding of ^{99m}Tc -teboroxime (18) to blood elements. Further stud-

ies in patients with coronary artery disease will be necessary to substantiate the variable washout rates of ^{99m}Tc -teboroxime described in dogs with coronary occlusions and pharmacologic stress (19).

A review of the clinical images reveals symmetric ^{99m}Tc -teboroxime uptake in normal subjects, whereas several cases of apparently decreased perfusion of the lateral wall have been noted with $^{13}\text{NH}_3$ in our experience with normals and as reported by others (20).

In conclusion, ^{99m}Tc provides an opportunity to study many of the new technetium compounds with PET. The potential applicability of these PET studies will be in the determination of the total uptake of radiopharmaceuticals by different organs as well as quantitation of differential washout rates in disease states. For the technetium radiopharmacologist, this opportunity offers a well-deserved window into the field of drug action.

ACKNOWLEDGMENTS

Supported by NIH grants CA 09206 and 1 R29 HL47003 FIRST award. The gift of CardioTec from Squibb Pharmaceuticals was greatly appreciated. The authors thank Dr. Karen Linder of Bristol Myers-Squibb for extensive consultations on technetium chemistry, Barb Mueller and Joni Hanson for technical support and the VA/UW Madison PET Center.

REFERENCES

1. Jurisson SS, Hirth W, Lindner KE, et al. Chloro \rightarrow hydroxy substitution on technetium BATO [$\text{TcCl}(\text{dioxime})_2\text{BR}$] complexes. *Nucl Med Biol* 1991;18:735-744.
2. Lederer CM, Shirley VS. *Table of isotopes*, 7th edition. New York: John Wiley and Sons; 1978:389.
3. Martin CC, Oakes TR, Nickles RJ. Small cyclotron production of Cu-60 PTSM for PET blood flow measurements [Abstract]. *J Nucl Med* 1980;31:815.
4. International Atomic Energy Agency. *Technical report #128*. Vienna: IAEA; 1971:705.

5. Molinski VJ. A review of Tc-99m generator technology. *Int J Appl Rad Isotopes* 1982;33:811-812.
6. Narra RK, Nunn AD, Kuczynski BL, Feld T, Wedeking P, Eckelman WC. A neutral technetium-99m complex for myocardial imaging. *J Nucl Med* 1989;30:1830-1837.
7. Till JE, Meyer HR, eds. *Radiological assessment, a textbook on environmental dose analysis*. Washington, DC: Office of Nuclear Reactor Regulation, US Nuclear Regulatory Commission, NUREG/CR-3332; 1983:7.61.
8. Snyder WS, Ford MR, Warner GG, et al. "S" absorbed dose per unit cumulated activity for selected radionuclides and organs. *MIRD pamphlet no. 11*. New York: Society of Nuclear Medicine; 1975.
9. Narra RK, Feld T, Nunn AD. Absorbed radiation dose to humans from technetium-99m-teboroxime. *J Nucl Med* 1992;33:88-93.
10. Nickles RJ, Christian BT, Martin CC, Nunn AD, Stone CK. Technetium-99m radionuclidic purity requirements for pharmacokinetic studies with PET [Abstract]. *J Nucl Med* 1992;33:850.
11. Wagner HN, ed. *Principles of nuclear medicine*. Philadelphia: WB Saunders; 1968.
12. Nickles RJ, Martin CC, Christian BT, Stone CK. Flow-through trapping to soften N-13-ammonia logistics [Abstract]. *J Nucl Med* 1992;33:931.
13. Martin CC. The kinetics of Cu-PTSM: a blood flow tracer for positron emission tomography. PhD thesis, Univ. of Wisconsin, Madison, 1992.
14. Lang TF, Hasegawa BH, Liew SC, et al. Description of a prototype emission-transmission computed tomography imaging system. *J Nucl Med* 1992;33:1881-1887.
15. Seldin DW, Johnson LL, Blood DK, et al. Myocardial perfusion imaging with technetium-99m-SQ30217: comparison with thallium-201 and coronary anatomy. *J Nucl Med* 1989;30:312-319.
16. Narra RK, Feld T, Wedeking P, Matyas J, Nunn AD, Coleman RE. SQ30217, a technetium-99m-labeled myocardial imaging agent which shows no interspecies differences in uptake. *Nuklearmedizin* 1987;23(suppl):489-491.
17. Clinical evaluation of SQ30217 as a myocardial imaging agent. Clinical Report 26742-I. New Brunswick, NJ: Squibb Diagnostics; 1986.
18. Rumsey WL, Rosenspire KC, Nunn AD. Myocardial extraction of teboroxime: effects of teboroxime interaction with blood. *J Nucl Med* 1992;33:94-101.
19. Stewaart RE, Heyle B, O'Rourke RA, Blumhardt R, Miller DD. Demonstration of differential post-stenotic myocardial technetium-99m-teboroxime clearance kinetics after experimental ischemia and hyperemic stress. *J Nucl Med* 1991;32:2000-2008.
20. Baudhuin T, Melin JA, Marwick T, et al. Regional uptake and blood flow variations with N-13 ammonia in normal subjects do not correlate with flow or metabolic measurements by other methods [Abstract]. *J Nucl Med* 1992;33:837.